THE JOURNAL OF PHYSICAL CHEMISTRY B

Article

Cite This: J. Phys. Chem. B 2019, 123, 2780−2791

pubs.acs.org/JPCB

Structure and Function of Tryptophan−Tyrosine Dyads in Biomimetic β Hairpins

Tyler G. McCaslin,[†,‡,♦] Cynthia V. Pagba,[†,‡,♦] San-Hui Chi,[†,§] Hyea J. Hwang,[∥] James C. Gumbart,[†,‡,⊥] Joseph W. Perry,[†,§] Cristina Olivieri,[#] Fernando Porcelli,[○] Gianluigi Veglia,[#,▽] Zhanjun Guo,[†,‡] Miranda McDaniel,[†,‡] and Bridgette A. Barry*[,†,‡]

[†]School of Chemistry and Biochemistry, [‡]The Parker H. Petit Institute of Bioengineering and Bioscience, [§]Center of Organic Photonics and Electronics, [∥]School of Materials Science and Engineering, and [⊥]School of Physics, Georgia Institute of Technology, Atlanta, Georgia 30332, United States

[#]Department of Biochemistry, Molecular Biophysics, and Biophysics and [▽]Department of Chemistry, University of Minnesota, Minneapolis, Minnesota 55455, United States

[○]Department for Innovation in Biological, Agro-Food and Forest Systems, University of Tuscia, 01100 Viterbo, Italy

Supporting Information

ABSTRACT: Tyrosine−tryptophan (YW) dyads are ubiquitous structural motifs in enzymes and play roles in proton-coupled electron transfer (PCET) and, possibly, protection from oxidative stress. Here, we describe the function of YW dyads in de novo designed 18-mer, β hairpins. In Peptide M, a YW dyad is formed between W14 and Y5. A UV hypochromic effect and an excitonic Cotton signal are observed, in addition to singlet, excited state (W*) and fluorescence emission spectral shifts. In a second Peptide, Peptide MW, a Y5−W13 dyad is formed diagonally across the strand and distorts the backbone. On a picosecond timescale, the W* excited-state decay kinetics are similar in all peptides but are accelerated relative to amino acids in solution. In Peptide MW, the W* spectrum is consistent with increased conformational flexibility. In Peptide M and MW, the electron paramagnetic resonance spectra obtained after UV photolysis are characteristic of tyrosine and tryptophan radicals at 160 K. Notably, at pH 9, the radical photolysis yield is decreased in Peptide M and MW, compared to that in a tyrosine and tryptophan mixture. This protective effect is not observed at pH 11 and is not observed in peptides containing a tryptophan−histidine dyad or tryptophan alone. The YW dyad protective effect is attributed to an increase in the radical recombination rate. This increase in rate can be facilitated by hydrogen-bonding interactions, which lower the barrier for the PCET reaction at pH 9. These results suggest that the YW dyad structural motif promotes radical quenching under conditions of reactive oxygen stress.

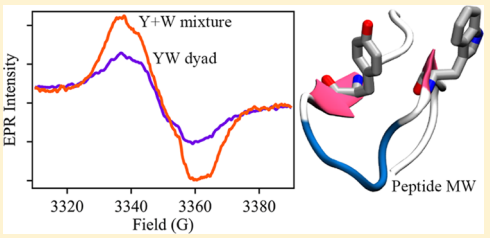

INTRODUCTION

Proton-coupled electron transfer (PCET) and electron transfer (ET) reactions are ubiquitous in biology and play essential roles in respiration, photosynthesis, and DNA synthesis.[1] In photosynthesis and DNA synthesis, these reactions involve the transient oxidation and reduction of the aromatic amino acids, tryptophan, and tyrosine. When produced in solution, these reactive aromatic species have microsecond lifetimes. However, the protein environment can stabilize the radicals and extend lifetimes out to the hours or days timescale.[2,3] In addition, cellular reactions involving oxygen can produce singlet oxygen species, which are potentially reactive and damaging to biological macromolecules. Cells have evolved mechanisms to avoid these deleterious side reactions of reactive oxygen, which can damage proteins (for examples, see refs4−6).

Tyrosine−tryptophan (YW) dyads are conserved structural motifs in a variety of oxidoreductases and other enzymes.[7,8] These dyads are identified as pairs or clusters of tyrosine−tryptophan side chains in which the inter-ring distance is less than 10 Å (for example, see ref 9). A conserved tyrosine−tryptophan dyad is found in class 1a ribonucleotide reductases (RNRs) (Figure 1A) and involves the tyrosyl radical initiator Y122• and W48 (*Escherichia coli* numbering).[10] In PSII, two redox-active tyrosines YD and YZ (Figure 1B−E)[11−13] conduct light-induced ET and PCET reactions via a hopping mechanism in photosynthetic oxygen evolution. The placement of tryptophan side chains near the two tyrosines YD and YZ distinguishes the two redox-active sites (Figure 1B−E). This is of interest because, although YZ is essential in function, YD forms a more stable radical, which persists in the dark for hours after illumination.[14]

Due to the wide distribution of the YW dyad motif in enzymes, it has been proposed that these dyads may serve a protective function, possibly by minimizing oxidative damage caused by reactive oxygen species (ROS). One protective mechanism could involve rapid radical transfer, through the

Received: December 26, 2018
Revised: February 17, 2019
Published: March 19, 2019

DOI: 10.1021/acs.jpcb.8b12452
J. Phys. Chem. B 2019, 123, 2780−2791

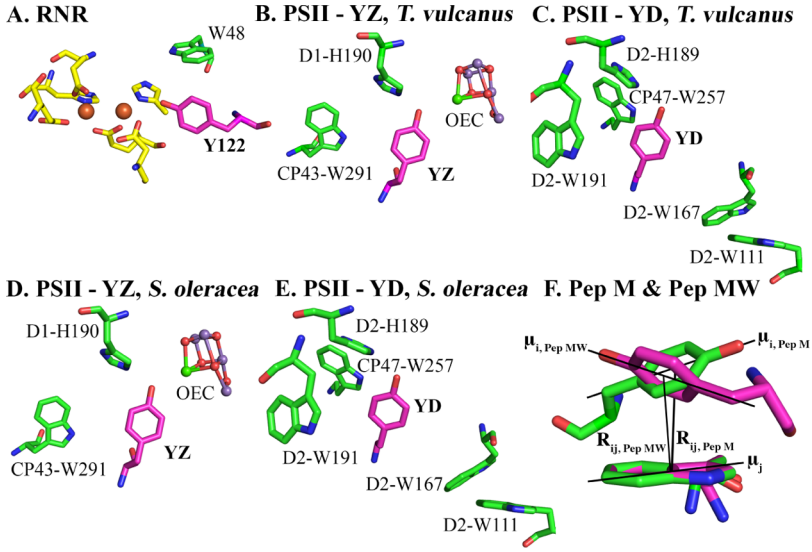

Figure 1. YW interactions in X-ray structures of RNR ((A) Y122, PDB 1MXR, ref 15), cyanobacterial (*Thermosynechococcus vulcanus*) PSII ((B) YZ and (C) YD, PDB 4UB6, ref 12), and spinach (*Spinacia oleracea*) PSII ((D) YZ and (E) YD, PDB 3JCU, ref 13). (F) shows dihedral angles between tyrosine and tryptophan transition moments ($\boldsymbol{\mu}_i$ and $\boldsymbol{\mu}_j$, respectively) and the inter-ring vector, $\mathbf{R}_{ij}$, in the lowest energy NMR structures of Peptide M (green) and Peptide MW (purple). The orientation of the transition moments is defined in refs16−18.

dyad, to the protein surface. At the surface, the oxidizing equivalents could be scavenged in cellular metabolism.[7,8] In this case, the rate at which oxidizing equivalents are transferred to the surface must be slower than the catalytic reaction. This mechanism could involve quenching of reactive oxygen species. Reactive oxygen is produced as a byproduct of UV damage and cellular reactions, which involve molecular oxygen. The production of hydroxyl, superoxide, and singlet oxygen is facilitated by the presence of metal ions and known to involve oxidative damage of tryptophan.[5,19] Tyrosine−tryptophan dyads could function as radical scavengers for these diffusive species.

To test the function of YW dyads in a structurally well-defined system, we have used 18-mer, de novo designed β hairpin peptides. Biomimetic peptide models or maquettes provide an incisive tool for studying noncovalent interactions (reviewed in ref 20). Previously, designed peptide and adapted protein models have been utilized to define the photochemical properties of tryptophan and tyrosine. For example, the fluorescence emission of tryptophan has been studied in engineered β hairpin peptides[21] and the ET properties of tryptophan have been studied in modified variants of azurin.[22] For tyrosine, redox properties and excited-state spectra have been reported for a β hairpin peptide, called Peptide A.[23,24] The PSII-inspired hairpin, Peptide A, contains tyrosine and histidine and conducts a proton transfer from tyrosine to histidine when the tyrosine is oxidized in the mid-pH range. The coupling of the PCET and ET reactions with conformational dynamics has been investigated in Peptide A with UV resonance Raman (UVRR) and molecular dynamics (MD) simulations.[25,26] Time-resolved spectroscopy has been used to investigate the effects of noncovalent interactions on ET and PCET kinetics.[27,28] The effect of a hydrophobic environment on PCET and ET of tyrosine has also been investigated in α helical peptides.[29−31]

UV resonance Raman (UVRR) studies of an RNR-inspired β-hairpin maquette, Peptide M, have also been reported previously. This peptide contains a single tyrosine and a single tryptophan, which exhibit dipole−dipole coupling. The unique UVRR spectrum of Peptide M was suggested to be characteristic of charge transfer between tyrosyl radical and tryptophan.[32] The UVRR spectrum of Peptide M was reported to be similar to the spectrum of the Y122−W48 in RNR.[33] Here, we use this peptide and its sequence variants to examine the broader role of the YW dyads in structure and function. The results suggest a role for dyads in structural stabilization and in radical scavenging.

MATERIALS AND METHODS

Peptides were synthesized by solid-phase synthesis (GenScript, Piscataway, NJ). NMR structures were determined using previously described methods.[23,32] Circular dichroism (CD) spectra were collected in a Peltier-type cell using a Jasco J-810 spectropolarimeter.[32] Electron paramagnetic resonance (EPR) spectroscopy was performed on a Bruker EMX spectrometer equipped with a liquid nitrogen cryostat. A frequency quadrupled Nd-YAG laser was used for photolysis (266 nm) methods.[23,32] Time-resolved absorption spectra (TRAS) were measured using a HELIOS spectroscopy system.[27,28] The system consisted of a regeneratively amplified Ti:sapphire laser (100 fs pulse width) and a computer-controlled optical parametric amplifier (OPA) pumped by the amplified laser. The 280 nm photolysis pulse was generated by the fourth harmonic of the OPA. Molecular dynamics simulations were performed using previously described methods.[26] A more detailed summary of methods and spectroscopic approaches is given in the Supporting Information (SI).

RESULTS

Sequences and NMR Structures. Figure S1, SI presents the primary sequences of the β-hairpin peptides investigated in this paper, named peptides M (B), MW (C), W (D), and WA14 (E). As a control in some experiments, Peptide A, was used (see Figure S1A, SI). Peptide A is a stably folded β hairpin.[23,24] Peptide A does not contain a YW dyad but is a tyrosine−histidine containing peptide. In the lowest energy NMR structures, Peptide A forms a β hairpin with a $\pi-\pi$

DOI: 10.1021/acs.jpcb.8b12452
J. Phys. Chem. B 2019, 123, 2780−2791

interaction between tyrosine (Y5) and histidine (H14) (Figure 2A). The average structure shows that A is stabilized by two

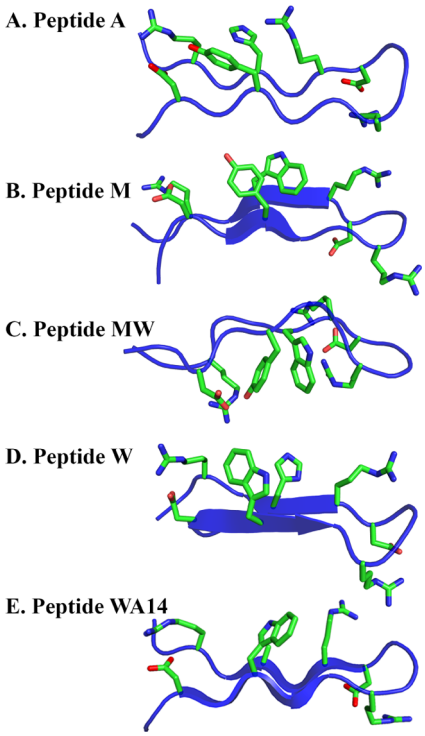

Figure 2. Lowest energy NMR structures of (A) Peptide A, (B) Peptide M, (C) Peptide MW, and (D) Peptide W. In (E), a PEP-FOLD[34] model of Peptide WA14.

D−R salt bridges and contains an arginine at position 12, which has a π−cation interaction with H14. Peptide M (see Figure S1B, SI) is a sequence variant of Peptide A, which is designed to contain a dyad and in which tryptophan has been substituted for H14 (W14).

Previously, we determined the NMR structure of Peptide M.[32] This structure shows that the Y5 and W14 aromatic rings do indeed interact as a dyad and exhibit a π−π interaction (Figure 2B and ref 32). Note that Y5 and W14 are not hydrogen bonded to each other in the lowest energy structure. In the sequence variant, Peptide MW (see Figure S1C, SI), the tryptophan side chain is placed at position 13, with an alanine substituted at position 14. The NMR structure of Peptide MW reported here reveals a folded β hairpin, in which Y5 and W13 form a dyad from opposite sides of the hairpin (Figure 2C). Peptide W contains a tryptophan substituted at position 5 and a histidine at position 14 (see Figure S1D, SI). The NMR structure of Peptide W confirms the formation of a WH interacting, cofacial pair in this peptide, formed from the same side of the β hairpin (Figure 2D). Peptide WA14 was used as a control; this peptide contains only one aromatic group, W5 (see Figure S1E, SI). Peptide WA14 forms a β hairpin (Figure 2E), as predicted by the program, PEP-FOLD.[34]

Figures 2 and S2−S5 (SI) provide a summary of the NMR data on these peptides and compare the results with the NMR structure of the original Peptide A. The orientation of the aromatic rings in Peptide M and MW is cofacial (Figures 2 and S2, SI). The cofacial arrangement and inter-ring distances are similar in the 20 lowest energy structures (see Figure S2, SI). The chemical shifts reflect the average of all of the possible conformations that are in solution. Although there is a population still folded as reflected by the dipolar contacts (see Figure S3, SI), in the mutated peptides, the folded population is lower. As shown in the chemical shift index (see Figure S4, SI), the chemical shifts change with the mutations. Table S1 (SI) summarizes the distance between aromatic groups in the lowest energy structures of Peptide MW (see Table S1A, SI), Peptide W (see Table S1B, SI), and Peptide M (see Table S1C, SI). In Peptide M, the average distance between the phenolic oxygen of Y5 and the indole nitrogen of W14 is ∼6 Å, as reported previously.[32] For Peptide MW, the average distance between the phenolic oxygen of Y5 and the indole nitrogen of W13 is ∼7 Å. W5 and H14 in Peptide W are measured to be ∼6 Å apart. Resonance assignments for Peptide W and Peptide MW are given in Tables S2 and S3 (SI), respectively. Table S4 (SI) shows the measured coupling constants for Peptide W and Peptide MW.

Molecular Dynamics Simulations. Simulations of Peptide M, MW, and W were conducted over 200 ns, repeated four times for each peptide (2.4 μs in total; Figure S6). Additionally, one 100 ns replica-exchange with solute tempering (REST2) simulation was run for each peptide (Figure 3), which allows for enhanced sampling at increased computational cost (see Materials and Methods, SI).[35,36] These simulations represent the charge state at pH 9, in which the

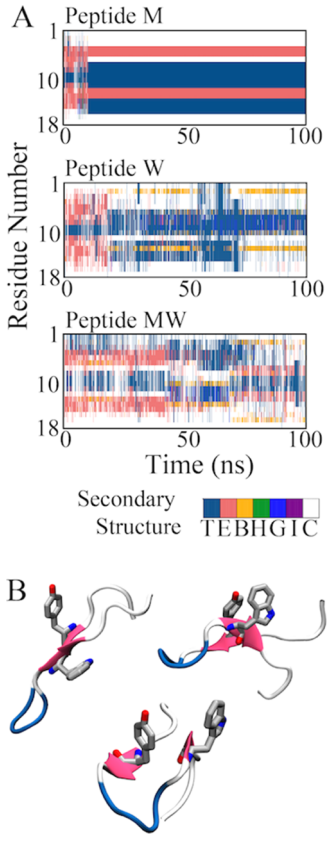

Figure 3. MD simulations of Peptide M, W, and MW. (A) Time evolution of secondary-structure assignment per residue of Peptide M (top), Peptide W (middle), and Peptide MW (bottom) during REST2 simulations. The legend uses DSSP classification: T is β turn, E is β sheet, B is β bridge, H is α helix, G is 3_{10} helix, I is π helix, and C is an unstructured coil. (B) Snapshots of the YW dyad structure in Peptide MW.

DOI: 10.1021/acs.jpcb.8b12452
J. Phys. Chem. B 2019, 123, 2780−2791

W and Y side chains are net neutral. The simulations of Peptide M are consistent with a stable folded structure in most of the simulation runs (Figure 3A). In Peptide MW, interactions between Y and W are formed and distort the peptide backbone (Figure 3B). Peptide W simulations are consistent with a stable folded structure in all four equilibrium simulation runs (Figure S6); however, in the REST2 run, the β-sheet is lost for most of the simulation, although the hairpin is still compact (Figure 3A). A summary of average distance and hydrogen bonding, as derived from the simulations, is presented graphically in Figure S7, SI. The distance between tryptophan and tyrosine or tryptophan and histidine is relatively invariant on the 200 ns timescale at pH 9. Simulations of Peptide M at pH 11 were also conducted; at this pH, the tyrosine side chain is deprotonated (see Figure S8, SI). The change in the charge state did not alter the results of the simulation when compared with Peptide M at pH 9.

CD and Excitonic Splitting. Figure 4 presents CD data derived from the β-hairpin peptides. For comparison, the signal from Peptide A (I, pink, solid line), derived at pH 9 and 20 °C, is presented. This signal exhibits negative ellipticity at 200 nm and is characteristic of a β hairpin. Similar results were obtained from Peptide M (IIA, purple, solid line) and Peptide MW (IIIA, black, solid line). After heating to 80 °C, negative ellipticity at 200 nm is lost in all three peptide samples (Figure 4I–III, dot-dashed lines). All samples refold reversibly with cooling back to 20 °C, as assessed by recovery of the CD signal (Figure 4I–III, dashed lines). A similar signal was also observed in Peptide W and WA14 at 20 °C and pH 9. We conclude that all peptides form thermally stable β hairpins at 20 °C.

We previously reported a CD-detected Cotton signal, derived from excitonic coupling within the YW dyad of Peptide M. This signal arises from coupling between the ^1B_b band of tryptophan and the ^1L_a band of tyrosine. The exciton splitting depends on the magnitude and directions of the transition dipole vectors, $\boldsymbol{\mu}_i$ and $\boldsymbol{\mu}_j$, and the interchromophore distance ($\mathbf{R}_{ij}$) vectors (Figure 1F) between the aromatic side chains.[16,17] This signal is apparent in Figure 4IIB, solid, which presents the difference CD signal between Peptide M and Peptide A. The Peptide M excitonic splitting is sensitive to melting (Figure 4IIB, dashed), consistent with loss of the excitonic interaction when the peptide unfolds. As observed in Figure 4IIIB, the difference spectrum derived from Peptide MW also exhibits an excitonic coupling signal (solid), which is sensitive to melting (dashed). Given the signal-to-noise ratio, the signal in Peptide MW is similar to the excitonic splitting found in Peptide M. This result indicates that the average electronic interaction between the tyrosine ^1L_a and tryptophan ^1B_b states is similar, when averaged over the solution conformers of Peptide M and MW.

UV–Vis Spectrum. The UV spectra of Peptides M, MW, W, and WA14 are compared to those of tryptophan and a tyrosine–tryptophan mixture in Figure S9I,II, SI. At the same concentration, the UV absorbance of the peptides is decreased. The 266 nm extinction coefficient of the peptides was therefore determined at pH 9 (see Figure S9IV, SI) and found to be reduced by approximately a factor of 2, relative to tryptophan, in all peptides (5000 M^{-1} cm^{-1} in tryptophan, average 2700 M^{-1} cm^{-1} in the peptides). Such hypochromism is well documented in nucleic acids and also alters the UV absorption bands of peptides and proteins. This effect has been attributed to exciton coupling (dipole–dipole), dipole-induced

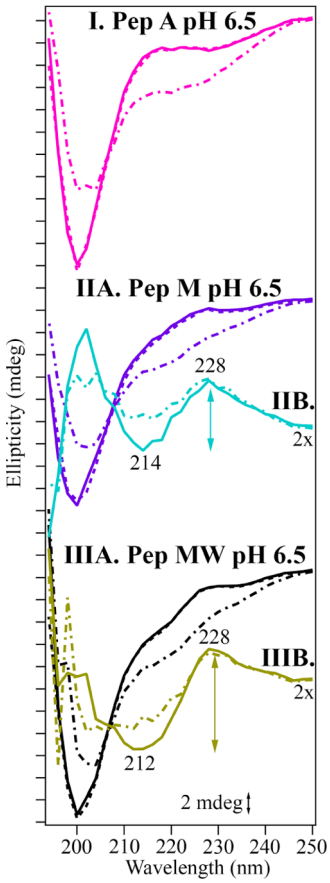

Figure 4. CD spectra of Peptide A (I, pink), Peptide M (IIA, purple), and Peptide MW (IIIA, black), pH 6.5. The spectra were acquired at 20 °C (solid line, premelt), 80 °C (dot-dashed line) or 20 °C (dashed line, postmelt). In (IIB), difference CD spectra are shown in cyan, corresponding to Peptide M (IIA, purple)-minus-Peptide A (I, pink). In (IIIB), difference CD spectra are shown in gold, corresponding to Peptide MW (III, black)-minus-Peptide A (I, pink). Data were obtained at 20 °C (IIB, cyan; IIIB, gold; solid line; premelt) or at 80 °C (IIB, cyan; IIIB, gold; dot-dashed line). Amplitude of the differential signal noted as a vertical line (IIB, cyan, 3.1 mdeg; IIIB, gold, 4.5 mdeg). Analyte concentration, 200 μm; buffer, 5 mM 2-(*N*-morpholino)ethanesulfonic acid, pH 6.5. The tick marks on the *y* axis denote 2 mdeg. Difference CD spectra (B, cyan and C, gold) are multiplied by a factor of 2 for presentation purposes.

dipole effects, and/or electrostatic effects.[37−39] After normalization to account for the difference in their extinction coefficients, red shifts of the Peptide M and MW spectra are observed, relative to tryptophan, Peptide W, and Peptide WA14 (see Figure S9III, SI). For Peptide M, this red shift was reported previously and attributed to a dipole–dipole interaction.[32] Note that previous work has shown that the peak potentials of the aromatic amino acids in Peptide M are similar to the peak potential of a mixture of aqueous tyrosine and tryptophan so the impact of dipole–dipole interactions in the ground and radical states must be compensating.[32]

Fluorescence Emission Spectrum. The fluorescence spectrum of tryptophan is known to be sensitive to the placement of charges near the indole ring.[40] For example, in crystallins, tryptophan–tryptophan interactions red shift the emission spectrum,[19] and it has been reported that electron transfer to the amide backbone can quench fluorescence.[41] To investigate any impact of the YW dyad on the fluorescence

DOI: 10.1021/acs.jpcb.8b12452
J. Phys. Chem. B 2019, 123, 2780−2791

emission spectrum, spectra of Peptide M and MW (see Figure S10A (SI), purple and black, respectively) were compared to those of an equimolar mixture of amino acids (orange), tyrosine in solution (blue), and tryptophan in solution (green) with fluorescence excitation at 266 nm. After correction for the extinction coefficient change in the peptides (see Figure S9IV, SI), there is little significant quenching of tryptophan fluorescence in the peptides, relative to the aqueous solution of tryptophan. However, tyrosine fluorescence is quenched in the YW dyad peptides; this effect is attributed to a Förster transfer from tyrosine to tryptophan in the dyad. In addition, the fluorescence emission spectrum of Peptide M (purple) is significantly blue shifted (5 nm), compared with a mixture of amino acids (orange), under the same conditions. The blue shift is observed at three different concentrations (see Figure S10B,C, SI), and Peptide MW (see Figure S10C, SI) behaved similar to Peptide M (see Figure S10B, SI). The blue shift is attributed to interaction between the π systems of Y and W in the dyad.

TRAS, Tryptophan and Tyrosine Amino Acid Solutions. Figure 5A presents TRAS, obtained from aqueous

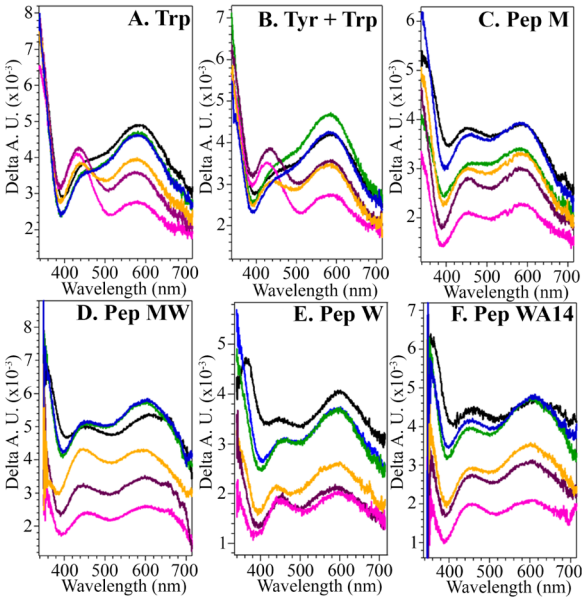

Figure 5. TRAS derived from (A) tryptophan, (B) a 1:1 mixture of tryptophan and tyrosine, (C) Peptide M, (D) Peptide MW, (E) Peptide W, and (F) Peptide WA14 after UV photolysis at pH 9. Spectra were obtained at 3 (black), 15 (blue), 33 (green), 513 (orange), 1033 (purple), and 2033 ps (pink). Analyte concentration, 1 mM; buffer, 5 mM borate-NaOH.

solutions of tryptophan after a femtosecond UV (280 nm) photolysis flash at pH 9.0. The spectra were acquired on the picosecond timescale, starting 3 ps (black) after the 280 nm pulse. The 3 ps spectrum (black) is dominated by three bands at ~360, 450, and 580 nm (Figure 5A). The band at 340 nm arises from the S_1 excited state of the indole ring in tryptophan. The 450 and 580 nm bands have also been assigned to the W* tryptophan excited state by picosecond spectroscopy and electronic structure calculations.[42] In the spectral region shown in Figure 5A, there are possible overlapping contributions from photoionization products, namely, the tryptophan cation radical at 580 nm and the tryptophan neutral radical at 510 nm. The pK_a of the tryptophan cation radical is 4.3; the deprotonation time is expected to be 10^{-6} s^{-1}, so the neutral radical is not expected to contribute on the picosecond timescale.[42] Similarly, formation of the triplet species, which absorbs at 430 nm, is not expected in oxygen-containing buffers on this timescale. The solvated electron makes a broad spectral contribution in the range from 650 to 700 nm.

Decay kinetics were monitored at selected wavelengths as a function of time, at 15 (blue), 33 (green), 513 (orange), 1033 (purple), and 2033 (pink) ps after the 280 nm flash. Biexponential fits and residuals are shown in Figure S11A, SI; the data are presented on a semilogarithm scale in Figure 6.

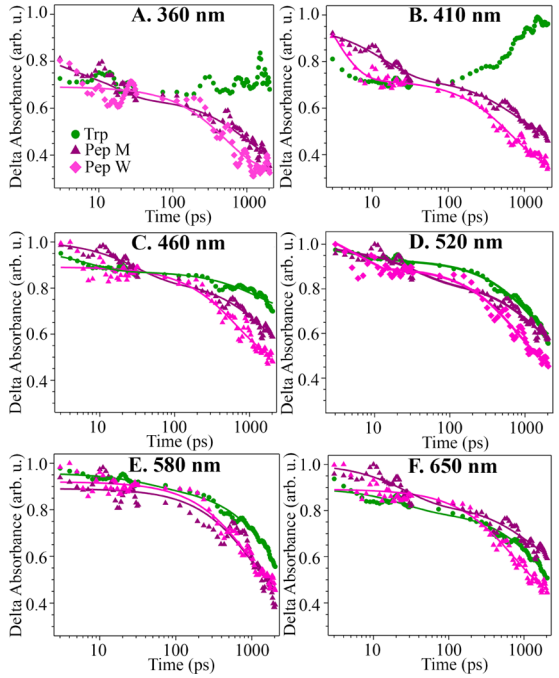

Figure 6. Decay kinetics obtained from TRAS of amino acid and selected peptides after UV photolysis at pH 9. Data were acquired from tryptophan (green), Peptide M (purple), and Peptide W (pink). Spectra were monitored at 360 nm (A), 410 nm (B), 460 nm (C), 520 nm (D), 580 nm (E), and 650 nm (F). Biexponential fits (starting from 3 ps) are superimposed as solid lines (see Table S5, SI). The averaged data were normalized with respect to the maximum absorbance, which occurred at 2−3 ps. A comparison of all kinetic data with residuals is shown in Figure S11, SI. Analyte concentration, 1 mM; buffer, 5 mM borate-NaOH.

On this timescale, the 360 nm band does not significantly decay in tryptophan (Figure 6A). The decay kinetics of the 520 nm band (Figure 6D) can be fit with a biexponential function with rate constants of 4 ps (4%) and 1000 ps (38%) (see Table S5, SI). Decay kinetics at 410, 460, 580, and 650 nm were also monitored (Figure 6B,C,E,F), and the wavelengths at which appreciable decay occurred were also fit with two exponentials. The need for two exponentials may be explained by a distribution of backbone conformers in solution.[43,44] The fits were consistent at all wavelengths, with fast phases in the 3−10 ps range and slow phases in the 1000−1900 ps range (see Table S5, SI). In tryptophan at pH 9, a new signal grows in on the 3 ps to 2 ns timescale (Figure 5A) as a band at 420 nm. Previously, this signal has been assigned to a photoproduct, produced as a result of indole ring protonation by the amino terminus of tryptophan.[45] TRAS and kinetic data were also derived from an aqueous mixture of tryptophan and tyrosine

DOI: 10.1021/acs.jpcb.8b12452
J. Phys. Chem. B 2019, 123, 2780−2791

(Figures 5B and S11B, SI). The bands and kinetics were indistinguishable when compared with those acquired from tryptophan alone, because spectral contributions derived from tyrosine are less intense compared with tryptophan (see Figures S12 and S13, SI). TRAS and kinetics were acquired from tryptophan at pH 11 (see Table S6, Figures S14, and S15, SI). The photoproduct was not formed at pH 11, as expected, because the amino group is not protonated.

TRAS, Peptides M, W, and WA14. Figure 5C shows TRAS data, obtained following a 280 nm excitation of a Peptide M sample, which contains a YW dyad. Bands at 360, 450, and 580 nm are observed at 3 ps, and overall, the peak positions are similar to those observed in aqueous tryptophan (Figure 5A) and the mixture of tryptophan and tyrosine (Figure 5B). In spectra acquired from Peptide M at pH 9, the 420 nm peak, characteristic of a photoproduct, does not appear. Kinetic data were derived from the Peptide M TRAS spectra after UV photolysis at pH 9 (see Figure S11C, SI). The TRAS data at 360, 410, 460, 520, 560, and 650 nm are shown on a semilog plot in Figure 6 and were fit with a biexponential function (see Table S5, SI). When compared to tryptophan, the 360 nm derived decay of W* is accelerated in Peptide M with time constants of 15 ps (14%) and 1000 ps (30%) (see Figure S11C and Table S5, SI). There are also changes when the kinetic fits are compared at other wavelengths (Figure 6). For example, at 520 nm, while Peptide M exhibited time constants of 33 ± 8 ps, 14%; 1500 ± 500 ps, 35%, the tryptophan sample yielded time constants of 4 ± 3 ps, 4%; 1000 ± 30, 38%. Notably, these changes on the picosecond timescale are not associated with a significant increase in fluorescence quenching in the peptide, as discussed above. TRAS and spectra were also obtained from Peptide M at pH 11 (see Figures S14 and S15, SI). At pH 11, the Peptide M sample exhibits mainly the 580 nm band at the 3 ps time point (see Figure S14B, SI). The decay kinetics in the peptide are accelerated relative to tryptophan in solution at this pH (see Figure S15, SI).

TRAS data were then obtained from Peptide W (Figure 5E). From the NMR structure, Peptide W is predicted to exhibit a tryptophan−histidine $\pi-\pi$ interaction. The spectra obtained on the picosecond timescale show changes in relative amplitudes of the 450 and 600 nm bands, when compared to spectra derived from Peptide M (Figure 5C). The decay is accelerated relative to tryptophan when analyzed at 360, 460, and 520 nm (Figures 6 and S11E, SI). Peptide WA14 (Figures 5F and S11F, SI) behaves similarly when compared to Peptide W (Figures 5E and S11E, SI). Both spectra and kinetics are similar to those of Peptide W. For example, fits to the 520 nm decay show that this peptide (see Table S5, SI) yields time constants of 1 ps (11%) and 780 ps (46%).

TRAS, Peptide MW. Peptide MW, which contains a YW dyad formed from opposite sides of the β strand, was examined using TRAS. In spectra derived on the picosecond timescale, Peptide MW (Figure 5D) exhibits a red shift of the ∼580 nm band, when compared to Peptide M (Figure 5C). Also, complex dynamics are observed in an evolution of the W* spectrum on the picosecond timescale (see Figure S16, SI). This spectral complexity is attributable to the conformational flexibility predicted by NMR spectroscopy and molecular dynamic simulations. The decay kinetics were monitored at various wavelengths, including 520 and 360 nm (see Figure S11D, SI). In Peptide MW, the W* decay kinetics are similar to the kinetics observed in Peptide M, Peptide W, and Peptide WA14 and are again faster than the decay kinetics observed in amino acid solutions (see Table S5, SI). Although the overall amount of decay at 2 ns does not change significantly, fits to the Peptide MW data show that only a small contribution from a fast phase (53 ps, 3%) is necessary to account for the data. Instead, the decay is dominated by a 1200 ps component, which is 59% of the amplitude. Changes in the time constants derived from biexponential fits may reflect average conformer selection in different peptide environments.

EPR Spectroscopy. To investigate any impact of the YW dyad on ET or PCET, EPR spectroscopy and UV photolysis were used to generate tryptophan and tyrosyl radicals in frozen aqueous samples at 160 K according to prior methods.[46] UV−vis absorption spectra were recorded before and after UV photolysis (see Figure S17, SI) and showed no significant changes to the spectrum, either in a mixture of tyrosine and tryptophan (see Figure S17A, SI) or in the peptides (see Peptide M for example, Figure S17B, SI). Figure S18A (SI) shows the result of an EPR spectrum recorded after a 266 nm UV photolysis (10 flashes) of tyrosine at pH 9. The spectrum is characteristic of a neutral tyrosyl radical. The tyrosyl radical EPR spectrum is dominated by coupling to the β-methylene protons and the 3,5-ring protons, with a g value of ∼2.004.[47] Figure S18E (SI) shows the results of photolysis of tryptophan at pH 9. The photochemistry of tryptophan is more complex than that of tyrosine, because the radical form of the indole side chain has a pK_a value of 4.3.[48] This complexity is evident when spectra at pH 4.3, 9, and 11 are compared (see Figure S19, SI). At pH 9 (see Figure S19B, SI), the spectrum corresponds to the neutral radical, $W^{\bullet}$. The EPR spectrum at pH 9 (see Figure S19B, SI) has a g value of 2.003, partially resolved hyperfine splittings, and an overall line width of ≥20 G. This spectrum is similar to that reported in the literature, and, at lower microwave power, exhibits the additional hyperfine splittings, which have been assigned to the β protons and the indole nitrogen.[49−51] At pH 4.3 (see Figure S19A, SI), the UV photolysis-induced spectrum is expected to reflect an approximately equal contribution from $WH^{\bullet+}$ and $W^{\bullet}$. At pH 4.3, the EPR signal (see Figure S19A, SI) has an overall 60 G line width, a g value of 2.006, and exhibits a new 1:1:1 splitting, which may represent a coupling to the indole nitrogen. The observed g value shift, when pH 4.3 and 9 are compared, is expected on the basis of previous studies of tryptophan radicals.[52,53] An additional experiment was performed to investigate the origin of the spectrum obtained at pH 9 in tryptophan (see Figure S19D, SI). As observed, UV photolysis at 160 K followed by warming to 200 K results in a g shift and the loss of a narrow g = 2.002 signal. At pH 11, the EPR spectrum is similar to the pH 9 spectrum, except for the superposition of a more intense g = 2.002 narrow signal (see Figure S19C, SI).

As expected, the EPR spectra of Peptide W (see Figure S18F, SI) and WA14 (see Figure S18G, SI) at pH 9 are similar to spectra acquired from tryptophan at the same pH (see Figure S18E, SI). EPR experiments were conducted on a 1:1 mixture of tyrosine and tryptophan (Figures 7A and S18B, SI). The EPR spectra of tyrosyl and tryptophan radicals are both produced in the mixture and overlap near g = 2 with a narrow signal (Figures 7A and S18B, SI). In Peptide M (Figures 7A and S18C, SI), UV photolysis produces a radical line shape that is similar but not identical to that in the mixture spectrum at pH 9 (see Figure S18, SI, inset). A similar result is obtained

DOI: 10.1021/acs.jpcb.8b12452
J. Phys. Chem. B 2019, 123, 2780−2791

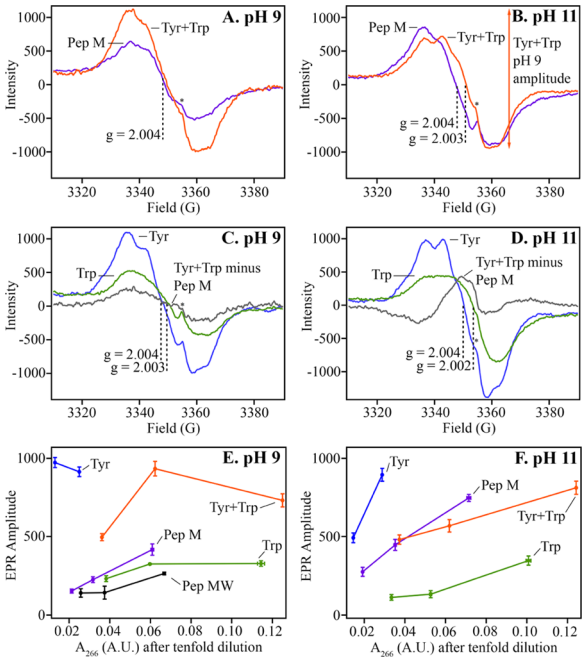

Figure 7. EPR spectra of peptides and amino acids at 160 K. In (A) and (B), EPR spectra derived after UV photolysis from a 1:1 tyrosine−tryptophan mixture (orange, 125 μm, A_{266} = 0.6) and Peptide M (purple, 250 μm, A_{266} = 0.6) at pH 9 (A) or pH 11 (B). In (C) and (D), the difference spectra, mixture-minus-Peptide M, at pH 9 (C) or pH 11 (D) are compared to EPR spectra derived from tyrosine (blue) and tryptophan (green) at the same pH. In (E) and (F), EPR amplitude at 3336 G, after subtraction of the zero offset at 3315 G, as a function of the measured 266 nm absorbance and after a 1-to-10 dilution, at pH 9 (E) or pH 11 (F). Samples: tyrosine (blue), a 1:1 molar mixture of tryptophan and tyrosine (orange), Peptide M (purple), Peptide MW (black), and tryptophan (green). Error bars represent the standard deviation of three to twelve replicate measurements. The asterisk marks a spectral artifact from the quartz EPR tube.

when Peptide MW is compared to the mixture (see Figure S18D, SI).

The amplitudes of the spectra acquired from Peptide M and the amino acid mixture at pH 9 are compared in Figure 7A. These spectra were derived from solutions with an equivalent 266 nm absorbance of 0.6 au (125 μm mixture; 250 μm Peptide M). The yield of radical appears to be decreased when Peptide M is compared to the mixture. At 3336 G (minus the baseline offset), the intensity of Peptide M is approximately 45% the intensity of the amino acid mixture at pH 9. To investigate this change in yield, the EPR amplitude is plotted versus a 266 nm absorption, as measured in each EPR sample after a 1-to-10 dilution (Figure 7E). These data confirm that the radical yield is decreased in Peptide M at pH 9 ((purple), when compared to that in the 1:1 mixture of tyrosine and tryptophan (orange). A similar decrease in yield is observed in Peptide MW, compared to that in the mixture at pH 9 (Figure 7E, black). Subtraction of the pH 9 spectra (mixture-minus-Peptide M) gives a difference spectrum that reflects a significant contribution from the tryptophan neutral radical (Figure 7C), which has a slightly larger, characteristic splitting compared to that of tyrosyl radical (see the annotation in Figure S18, SI). Subtractions using the pH 9 Peptide MW spectra gave a similar line shape. Note that in peptide W (see Figure S18II, SI, teal) and peptide WA14 (yellow), which lack the tyrosine, the radical yield is similar to the yield obtained in tryptophan alone (green). Importantly, at pH 11, the peptide M protective effect on radical yield is not observed. At 3336 G, the intensity in the mixture is similar (76%) to the intensity in peptide M (Figure 7B,F). Moreover, at pH 11, the difference spectrum, generated from the mixture and the peptide, resembles mainly a narrow radical (Figure 7D). The results are consistent with the conclusion that peptide M lowers the barrier for radical recombination at 160 K and pH 9 (see Discussion below).

DISCUSSION

This work defines the spectroscopic and functional impact of interaromatic interactions in a pair of YW dyads. The structural effects of aromatic−aromatic interactions in β hairpin model peptides have been investigated previously.[54] For example, in octamer β hairpins,[55] NMR analysis revealed side-chain interactions between the tyrosine and tryptophan rings even at nonhydrogen bonding sites and in organic solvents. In another study, aromatic edge-to-face-interactions were found to have a stabilizing effect on the free energy of β hairpins.[56] In a third example, time-resolved infrared spectroscopy was used to probe the effect of tryptophan mutagenesis in trpzip2 β hairpins.[57] These stabilizing effects of aromatic−aromatic interactions occur in globular proteins. For example, in proteins, it has been concluded that 60% of aromatic residues are involved in aromatic pairs, the majority of which form networks of three or more aromatic side chains.[58] Phenyl ring centroids are typically separated by 4.5−7 Å, and dihedral angles of approximately 90° are preferred. The contribution of these interactions to the free energy was deduced to depend on the environment but varied from 0.6 to 2 kcal/mol.

The YW aromatic−aromatic dyad is a structural motif found in many enzymes, particularly oxidoreductases.[7,8] They are likely to hold functional significance, as evident in the examination of two proteins, photosystem II and RNR (Figure 1). In RNR, Y122 in the β subunit acts as a catalytic initiator (reviewed in ref 59). In the absence of the α subunit, Y122 forms a stable radical. The X-ray structure of the singlet state shows that the tyrosine is in close proximity to the β subunit residue, W48.[15] Mutation shows that W48 plays an important role in RNR, in particular, in the assembly of the tyrosyl radical-diferric cluster.[59,60] In photosystem II, there are two redox-active tyrosines, YZ and YD (Y161 of the D1 subunit and Y160 of the D2 subunit, respectively), with different functional roles.[20] The YD radical forms a stable neutral tyrosyl radical with a lifetime on the hours timescale.[61] Mutagenesis of this tyrosine leads to a decrease in the steady-state rate of oxygen evolution, but the sample is not completely inactivated. It has been proposed that YD may be important in maintaining a high oxidation state of manganese in the active site. On the other hand, YZ is an essential electron transfer intermediate between the primary donor and the metal cluster with a microsecond to millisecond radical lifetime.[62,63] The environment of YZ contains one tryptophan, whereas that of YD has multiple interactions with tryptophan residues at interaction distances of ∼10 Å[11−13] (Figure 1). Interestingly, these interactions are observed both in cyanobacterial and spinach PSII structures.[12,13]

It has been suggested that YW dyads may act as defusers or radical scavengers. In this proposal, the YW dyads catalyze inter-ring electron transfer and conduct excess oxidizing equivalents from catalytic sites to the protein surface.[7,8]

DOI: 10.1021/acs.jpcb.8b12452
J. Phys. Chem. B 2019, 123, 2780−2791

Inter-ring transfer is possible, depending on orientation and midpoint potential of the tyrosine and tryptophan. Tyrosine has a pH-independent midpoint potential above the phenolic oxygen pK_a (~10) and has a midpoint potential that varies linearly with pH below this pK_a. Tryptophan can function either in ET or PCET in proteins.[48] Between pH 4 and 10, the midpoint potential of the neutral tryptophan radical is more positive than that of tyrosine.[48] For example, at pH values between 6 and 10, the neutral tryptophan radical oxidized tyrosine in dipeptides.[48] In azurin, it was also concluded that a W radical could be reduced by tyrosine.[22] For an intra-dyad ET or PCET reaction to be protective, the rates of these defusing reactions must be less than those of the catalytic reactions.

Here, we examine de novo designed, YW dyad-containing peptides in which the Y and W rings are in the range of 6−7 Å apart. A significant YW interaromatic interaction is evident from our CD experiments on the YW dyad-containing peptides. Tryptophan has multiple singlet excited states, termed B_a, B_b, L_a, and L_b, with absorption maxima of 195, 218, and 278 nm at pH 7.[64] A far UV CD signal is characteristic of excitonic splitting between the ^1B_b band of tryptophan and the ^1L_a band of tyrosine.[65] Previously, such excitonic coupling between tryptophans has been modeled in 12-mer model peptides using time-dependent density functional calculations.[18] In addition, a tyrosine−tryptophan excitonic signal has been observed previously in the protein, PagP.[17] To give rise to the CD signal of Peptide M and MW, the ^1L_a and ^1B_b states of tyrosine and tryptophan, respectively, must couple to give two excited states. The splitting energy, Δ_{ij},[17] equals $(\delta_{ij}^2 + 4V_{ij}^2)^{1/2}$, where V_{ij} is the interaction energy. The difference in transition energy, δ_{ij}, is calculated from the positive and negative components of the spectrum (σ_i and σ_j) and corresponds to 228 and 214/212 nm in our spectra of Peptide M and MW. V_{ij} is calculated from the dipole−dipole interaction between the transition dipole moments ($\boldsymbol{\mu}$) and equals

$$V_{ij} = \boldsymbol{\mu}_i \cdot \boldsymbol{\mu}_j / |R_{ij}^3| - 3(\boldsymbol{\mu}_i \cdot \mathbf{R}_{ij})(\boldsymbol{\mu}_j \cdot \mathbf{R}_{ij}) / |R_{ij}^5|$$

in which the bold face symbols denote vectors (Figure 1F).

The rotational strength, R_o, which is the amplitude of the signal, depends on the triple product.

$$R_0 = \pm\pi\ V_{ij}(\sigma_i\ \sigma_j)^{1/2}[\mathbf{R}_{ij} \cdot (\boldsymbol{\mu}_i \times \boldsymbol{\mu}_j)]/\Delta_{ij}$$

In the NMR structures of Peptide M and MW, the tyrosine phenolic group is oriented in opposite directions, relative to the indole ring (Figure 1F). One component of the tyrosine transition dipole moment is oriented along this CO bond.[17] The tryptophan transition dipole moment is oriented parallel to the long dimension of the indole ring, bisecting the ring system.[18] Use of the dihedral angles derived from the lowest energy NMR structures (Figure 1F) predicts that the value of V_{ij} will be within a factor of 2 when Peptide M and MW are compared. This is in agreement with the observed Cotton signal amplitudes.

The UV absorption band, assignable to $^1L_{a/b}$, is red-shifted in Peptide M and MW. The fluorescence emission spectrum of the YW dyad peptides is also shifted. In proteins, tryptophan fluorescence occurs mainly from the singlet L_a state with a lifetime in the nanosecond time regime.[66] The fluorescence yield varies dramatically in proteins.[41] We show here that the YW dyad has the effect of blue-shifting the fluorescence emission spectrum of W by approximately 5 nm. Negative charges near the benzene ring or positive charges near the pyrrole ring are expected to shift the emission to shorter wavelengths.[40] In the lowest energy NMR structures of Peptide M and MW, the nearest functional group to the tryptophan ring is the phenol moiety. Specifically, Y5 is positioned with π electron density proximal to the benzene portion of the indole ring. On the basis of the lowest energy NMR structures, the nearest C−C distances from Y5 to W14 (Peptide M) or W13 (Peptide MW) are 3.0 and 2.9 Å, respectively. Therefore, the YW interaction can account for the fluorescence emission blue shift. We also find that fluorescence emission from the tyrosine phenol ring is quenched in the YW dyad-containing peptides. This is attributable to a Förster dipole−dipole transfer mechanism between the tryptophan and tyrosine rings. Although quenching of tryptophan fluorescence via electron transfer can also sometimes be observed in tryptophan-containing proteins[41,67] and peptides,[21] we show that quenching of the tryptophan fluorescence is not significant in Peptide M and MW. The amount of quenching will depend on the electronic coupling and the energy gap, and these factors are sensitive to the detailed protein environment.

We measured the spectra and lifetime of the W* produced in peptide and aqueous amino acid samples after UV photolysis on the picosecond timescale.[27,28] The spectra are dominated by contributions from the S_1 excited state of the indole ring, W*. This W* decays by multiple mechanisms, which include photoproduct formation, electron transfer, and other mechanisms. Photoionization is expected and is accompanied by production of a solvated electron with absorption at 650 nm, as observed here. The formation of the W* signal is complete in 3 ps, and the solvated electron signal decays on the picosecond timescale. The spectra that we report from tryptophan and tryptophan−tyrosine mixtures are similar to previous reports of the indole S_1 excited state, with absorption at 345/360 and 520 nm.[42,45,68,69] In tryptophan and in the mixture, the formation of a H^+ indole photoproduct is also evident as a 420 nm spectral feature that grows in ~500 ps. The source of the proton has been attributed to the tryptophan amino group.[45,68] This photoproduct is not observed in the peptide samples studied here. The lifetime of the W* state in tryptophan, as reported here, is consistent with previous reports of the nanosecond fluorescence lifetime of tryptophan.[42,45,68,69]

The TRAS data acquired on the picosecond timescale show that the excited spectra of Peptide M, MW, W, and WA14 are all distinguishable by minor intensity changes at 450 and 600 nm. These are most likely attributable to changes in electrostatic interactions in the peptides. In addition, the spectrum of Peptide MW is red-shifted when compared to Peptide M or tryptophan and exhibits complex spectral changes on the picosecond timescale. This red shift and the picosecond-time-dependent alterations are attributed to the unique conformational landscape sampled by this peptide. We conclude that the structural relaxation in Peptide MW influences the S_1 excited-state surface and reflects the detailed arrangement of charged groups near the indole ring. Note that the excited-state spectrum of Peptide M is pH dependent, indicating that the deprotonation state of amino acid side chains is an important determinant in this process.

The decay rate of the W* state is similar in all four peptides. However, the rate observed in the peptides is accelerated, when compared to that in tryptophan solutions or

DOI: 10.1021/acs.jpcb.8b12452
J. Phys. Chem. B 2019, 123, 2780−2791

tryptophan–tyrosine mixtures. For example, at 360 nm, there is no appreciable signal decay in an aqueous solution of tryptophan; however, significant spectral decay is observed in all peptides on the picosecond timescale. This is a wavelength at which tyrosine excited-state decay makes no significant contribution. Because this acceleration is independent of the tryptophan's noncovalent interactions, the effect is attributable to the influence of the peptide backbone. The tryptophan radical can decay by recombination with the solvated electron.[39,48] The tryptophan radical is most likely formed with 280 nm photolysis on the 2 ns timescale, even if not directly detected under the intense W* absorption, because our spectra provide evidence for the production of a solvated electron. Previous studies of tyrosyl radical decay in β hairpins have demonstrated a peptide backbone-induced increase in PCET and ET rate, which alters the rate of radical recombination. In that case, this increase in decay rate was attributed to an increase in electronic coupling.[27,28] Such an increase in electronic coupling can accelerate the rate of tryptophan radical decay in Peptide M and thus accelerate W* decay, as well.

To test if the YW dyads in the β hairpins have unique electron and proton transfer characteristics, radical yield was measured using EPR spectroscopy after UV photolysis at 160 K. UV photolysis can produce reactive oxygen species, which leads to damage of the indole ring. Such oxidative damage may alter the UV spectrum and is expected to be evident in spectra obtained from tryptophan solutions after UV laser flashes. However, in our experiments, the spectra acquired from tryptophan-containing peptides or the tyrosine–tryptophan mixture were not significantly altered by UV photolysis. The 266 nm flash is expected to generate a neutral radical in tyrosine and tryptophan solutions at pH 9. This was confirmed by comparison of radical line shapes produced at pH 4.3, 9.0, and 11.0 in tryptophan.

At pH 9.0, the radical yield is substantially reduced in Peptide M and MW, when compared to that in a mixture of tyrosine and tryptophan. The majority of the pH 9 effect appears to be on the yield of tryptophan radical, as assessed from the difference spectrum. However, significantly, at pH 11, the yield of neutral tryptophan radical, $W^{\bullet}$, is similar in Peptide M, when compared to that in a 1:1 mixture. Notably, MD simulations of Peptide M indicate that the structure of the peptide at pH 11 is similar to the structure at pH 9. In addition, at pH 9.0, the yield of $W^{\bullet}$ is indistinguishable in peptides W and WA14, when compared with the radical yield in tryptophan.

In UV flash photolysis, the radical yield equals the number of radicals formed per number of photons absorbed. The number of photons absorbed in dilute solution is linearly proportional to the absorbance at 266 nm, the path length, and concentration. With the path length and incident intensity held constant, a plot of amplitude versus the 266 nm absorption shows a quenching effect specific to Peptide M and MW. What is the origin of this quenching effect at pH 9? The effect could be on the formation rate or on the recombination rate. Because the tyrosyl and tryptophan radicals are formed in the excited state, alterations in the description of the S_1 excited state or in the rates of S_1 decay, internal conversion, and radical formation could impact the EPR yield. The TRAS and kinetic experiments provide evidence that the S_1 excited states decay more slowly in the amino acid mixture, compared with the peptides. This could contribute to a difference in yield; however, the effect on the excited-state decay rate was observed both at pH 9 and 11 and was observed in peptides in which no protective effect was detected (Peptide W and WA14). Therefore, a change in the formation rate due to alterations in the excited state seems an unlikely explanation of Peptide M radical quenching in the EPR experiment. In addition, fluorescence experiments confirm that the YW dyad has little effect on tryptophan fluorescence quenching. Note that the midpoint potential of Peptide M is similar to that of amino acids.[32]

On the basis of the considerations above, we propose that the protective effect observed on radical yield in Peptide M and MW is due to alteration in the radical recombination rate at pH 9 (Figure 8). Tyrosyl radicals decay by recombination

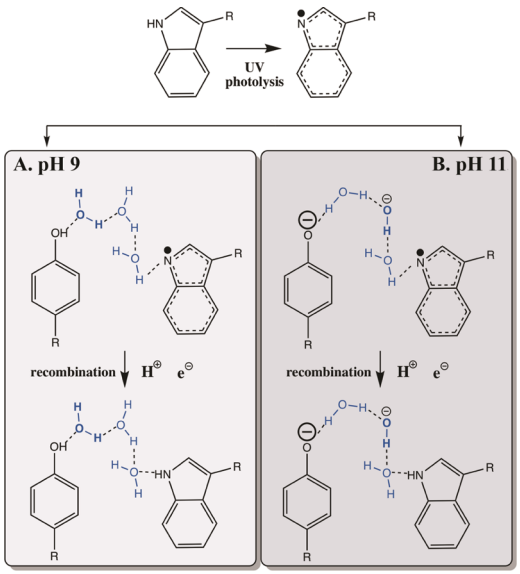

Figure 8. Schematic illustrating UV photolysis, radical generation, a pH-induced change in a hydrogen bonding network containing Y and W, and a speculative protective mechanism in the YW dyad-containing peptides.

with the solvated electron and a proton at pH 9 but with solvated electron alone at pH 11. Tryptophan neutral radical decays by a PCET reaction, involving H^+ and e^-, at both pH values. From the EPR difference spectra of Peptide M and MW, the majority of the protective effect appears to be on tryptophan radical. At pH 9, the tyrosine side chain is protonated and the protective effect can be attributed to rapid PCET through a hydrogen-bonding network, which contains the tyrosine and hydrogen-bonded water molecules (Figure 8). Consistent with the role for this protonated tyrosine side chain, there is no significant effect on yield when Peptides W and WA14 are compared to tryptophan. Also, the YW protective effect is not evident at pH 11, where the negative charge on the tyrosinate may disrupt hydrogen-bonding interactions (Figure 8). This speculative model proposes that the interactions of the YW side chains with nearby water molecules are important kinetically and lower a barrier for PCET. A similar model has been proposed to explain PCET reactions in a DNA photolyase[70] and in donor–acceptor supramolecules assembled through a hydrogen bonded interface (reviewed in ref 71).

Previous studies of azurin have provided evidence that the presence of tyrosine in the protein can quench a stable

DOI: 10.1021/acs.jpcb.8b12452
J. Phys. Chem. B 2019, 123, 2780–2791

tryptophan radical. This was attributed to intramolecular ET from tyrosine to the tryptophan radical.[22] A similar process has been proposed to rationalize the UV spectrum of Peptide M by another group.[32] In DNA photolyase from *Anacystis nidulans*, a microsecond ET pathway was proposed to involve a tyrosine-to-tryptophan radical transfer step but only in ∼40% of the sample.[53] However, tyrosine-to-tryptophan radical ET is not a consistent explanation of our EPR results, because oxidation of tyrosine at the expense of tryptophan radical would still generate an overlapping $g = 2$ radical and would not decrease the overall intensity of the EPR spectrum in Peptide M and MW at pH 9. Instead, we favor the explanation that the barrier for radical recombination with the solvated electron is decreased.

Distances of 6−7 Å, as found here in Peptide M and MW, have been described in extensive aromatic wires in cytochrome *c* oxidase and human superoxide dismutase. In PSII and RNR, the Y−W distance is ∼10 Å (Figure 1A−E). Whereas distances of 10 Å are expected to support electron exchange on the microsecond timescale ($\Delta G = 0$, $\lambda = 1$ eV, $T = 295$ K), distances of 7.5 Å have been proposed to support much faster ET rates.[7,8] In cyanobacterial and spinach PSII (Figure 1B,D), YZ interacts at a distance of ∼10 Å with a single tryptophan and decays on the microsecond−millisecond timescale. YD (Figure 1C,E) has multiple tryptophan interactions predicted at 10 Å and decays on the hour timescale. Y122 radical in the isolated *E. coli* RNR β subunit is stable for days in the singlet structure, Y122 is ∼10 Å from a surface-exposed tryptophan (Figure 1A). The reason for these distinctions in stability is not known but has been proposed to be due to access of water to the radical site.[33] This comparison underlines the importance of modeling YW interactions at distinct OH−N distances and orientations.

CONCLUSIONS

The distribution and prevalence of YW dyads in enzymes suggest that solvent-exposed dyads and aromatic clusters play important roles in structure and function. Here, we show that the energetics of a YW aromatic interaction is sufficient to destabilize the backbone fold and to introduce spectrally detectable, conformational dynamics on the picosecond timescale. The peptide backbone is observed to accelerate the rate of W* decay. We also provide evidence that peptides, containing these YW dyads, exhibit a decreased yield of free radicals after UV photolysis at pH 9. These results support a protective role for YW dyads (6−7 Å distances) as ROS scavengers and free-radical quenchers.

ASSOCIATED CONTENT

Supporting Information

The Supporting Information is available free of charge on the ACS Publications website at DOI: 10.1021/acs.jpcb.8b12452.

Distances derived from NMR structures, kinetic constants derived from biexponential fits to the TRAS data, NMR structures and data, results from molecular dynamics simulations, UV−vis spectra, fluorescence spectra, TRAS spectra and kinetics at pH 9 and 11, UV−vis spectra before and after EPR measurements, and EPR spectra (PDF)

AUTHOR INFORMATION

Corresponding Author

*E-mail: bridgette.barry@chemistry.gatech.edu. Phone: 404-385-6085.

ORCID

James C. Gumbart: 0000-0002-1510-7842
Joseph W. Perry: 0000-0003-1101-7337
Fernando Porcelli: 0000-0003-3209-0074
Bridgette A. Barry: 0000-0003-3421-1407

Author Contributions

♦T.G.M. and C.V.P. contributed equally to this work.

Notes

The authors declare no competing financial interest.

ACKNOWLEDGMENTS

This work was supported by NSF CLP 18-01926 (B.A.B), NIH GM-100310 (G.V.), and NSF MCB-1452464 (J.C.G.). T.G.M. was partially supported by the Georgia Tech GAANN program in Molecular Biophysics and Biotechnology. Computational resources were provided via the Extreme Science and Engineering Discovery Environment (XSEDE), which is supported by NSF grant number OCI-1053575.

REFERENCES

(1) Dempsey, J. L.; Winkler, J. R.; Gray, H. B. Proton-Coupled Electron Flow in Protein Redox Machines. *Chem. Rev.* **2010**, *110*, 7024−7039.

(2) Keough, J.; Jenson, D. L.; Zuniga, A.; Barry, B. A. Proton Coupled Electron Transfer and Redox-Active Tyrosine Z in the Photosynthetic Oxygen Evolving Complex. *J. Am. Chem. Soc.* **2011**, *133*, 11084−11087.

(3) Keough, J.; Zuniga, A.; Jenson, D. L.; Barry, B. A. Redox Control and Hydrogen Bonding Networks: Proton-Coupled Electron Transfer Reactions and Tyrosine Z in the Photosynthetic Oxygen-Evolving Complex. *J. Phys. Chem. B* **2013**, *117*, 1296−1307.

(4) Kasson, T. M.; Barry, B. A. Reactive Oxygen and Oxidative Stress: N-Formyl Kynurenine in Photosystem II and Non-Photosynthetic Proteins. *Photosynth. Res.* **2012**, *114*, 97−110.

(5) Ehrenshaft, M.; Deterding, L. J.; Mason, R. P. Tripping up Trp: Modification of Protein Tryptophan Residues by Reactive Oxygen Species, Modes of Detection, and Biological Consequences. *Free Radicals Biol. Med.* **2015**, *89*, 220−228.

(6) Taylor, R. M.; Sallans, L.; Frankel, L. K.; Bricker, T. M. Natively Oxidized Amino Acid Residues in the Spinach Cytochrome B_6F Complex. *Photosynth. Res.* **2018**, *137*, 141.

(7) Gray, H. B.; Winkler, J. R. Hole Hopping through Tyrosine/Tryptophan Chains Protects Proteins from Oxidative Damage. *Proc. Natl. Acad. Sci. U.S.A.* **2015**, *112*, 10920−10925.

(8) Winkler, J. R.; Gray, H. B. Could Tyrosine and Tryptophan Serve Multiple Roles in Biological Redox Processes? *Philos. Trans. R. Soc., A* **2015**, *373*, No. 20140178.

(9) Bradley, J. M.; Svistunenko, D. A.; Moore, G. R.; Le Brun, N. E. Tyr25, Tyr58 and Trp133 of *Escherichia coli* Bacterioferritin Transfer Electrons between Iron in the Central Cavity and the Ferroxidase Centre. *Metallomics* **2017**, *9*, 1421−1428.

(10) Nordlund, P.; Sjöberg, B.-M.; Eklund, H. Three-Dimensional Structure of the Free Radical Protein of Ribonucleotide Reductase. *Nature* **1990**, *345*, 593−598.

(11) Umena, Y.; Kawakami, K.; Shen, J.-R.; Kamiya, N. Crystal Structure of Oxygen-Evolving Photosystem II at a Resolution of 1.9 Angstrom. *Nature* **2011**, *473*, 55−60.

(12) Suga, M.; Akita, F.; Hirata, K.; Ueno, G.; Murakami, H.; Nakajima, Y.; Shimizu, T.; Yamashita, K.; Yamamoto, M.; Ago, H.; et al. Native Structure of Photosystem II at 1.95 Å Resolution Viewed by Femtosecond X-Ray Pulses. *Nature* **2015**, *517*, 99−103.

DOI: 10.1021/acs.jpcb.8b12452
J. Phys. Chem. B 2019, 123, 2780−2791

(13) Wei, X.; Su, X.; Cao, P.; Liu, X.; Chang, W.; Li, M.; Zhang, X.; Liu, Z. Structure of Spinach Photosystem II-LHCII Supercomplex at 3.2 Angstrom Resolution. *Nature* **2016**, *534*, 69−74.
(14) Barry, B. A. Proton Coupled Electron Transfer and Redox Active Tyrosines in Photosystem II. *J. Photochem. Photobiol., B* **2011**, *104*, 60−71.
(15) Högbom, M.; Galander, M.; Andersson, M.; Kolberg, M.; Hofbauer, W.; Lassmann, G.; Nordlund, P.; Lendzlan, F. Displacement of the Tryosyl Radical Cofactor in Ribonucleotide Reductase Obtained by Single-Crystal High-Field EPR and 1.4-Å X-Ray Data. *Proc. Natl. Acad. Sci. U.S.A.* **2003**, *100*, 3209−3214.
(16) Grishina, I. B.; Woody, R. W. Contributions of Tryptophan Side Chains to the Circular Dichroism of Globular Proteins: Exciton Couplets and Coupled Oscillators. *Faraday Discuss.* **1994**, 245−262.
(17) Khan, M. A.; Neale, C.; Michaux, C.; Pomes, R.; Prive, G. G.; Woody, R. W.; Bishop, R. E. Gauging a Hydrocarbon Ruler by an Intrinsic Exciton Probe. *Biochemistry* **2007**, *46*, 4565−4579.
(18) Roy, A.; Bour, P.; Keiderling, T. A. TD-DFT Modeling of the Circular Dichroism for a Tryptophan Zipper Peptide with Coupled Aromatic Residues. *Chirality* **2009**, *21*, E163−E71.
(19) Schafheimer, N.; King, J. Tryptophan Cluster Protects Human GammaD-Crystallin from Ultraviolet Radiation-Induced Photoaggregation *In Vitro*. *Photochem. Photobiol.* **2013**, *89*, 1106−1115.
(20) Barry, B. A. Reaction Dynamics and Proton Coupled Electron Transfer: Studies of Tyrosine-Based Charge Transfer in Natural and Biomimetic Systems. *Biochim. Biophys. Acta, Bioenerg.* **2015**, *1847*, 46−54.
(21) McMillan, A. W.; Kier, B. L.; Shu, I.; Byrne, A.; Andersen, N. H.; Parson, W. W. Fluorescence of Tryptophan in Designed Hairpin and Trp-Cage Miniproteins: Measurements of Fluorescence Yields and Calculations by Quantum Mechanical Molecular Dynamics Simulations. *J. Phys. Chem. B* **2013**, *117*, 1790−1809.
(22) Larson, B. C.; Pomponio, J. R.; Shafaat, H. S.; Kim, R. H.; Leigh, B. S.; Tauber, M. J.; Kim, J. E. Photogeneration and Quenching of Tryptophan Radical in Azurin. *J. Phys. Chem. B* **2015**, *119*, 9438−9449.
(23) Sibert, R.; Josowicz, M.; Porcelli, F.; Veglia, G.; Range, K.; Barry, B. A. Proton-Coupled Electron Transfer in a Biomimetic Peptide as a Model of Enzyme Regulatory Mechanisms. *J. Am. Chem. Soc.* **2007**, *129*, 4393−4400.
(24) Sibert, R. S.; Josowicz, M.; Barry, B. A. Control of Proton and Electron Transfer in *De Novo* Designed, Biomimetic Beta Hairpins. *ACS Chem. Biol.* **2010**, *5*, 1157−1168.
(25) Pagba, C. V.; Barry, B. A. Redox-Induced Conformational Switching in Photosystem-II-Inspired Biomimetic Peptides: A UV Resonance Raman Study. *J. Phys. Chem. B* **2012**, *116*, 10590−10599.
(26) Hwang, H.; McCaslin, T. G.; Hazel, A.; Pagba, C. V.; Nevin, C. M.; Pavlova, A.; Barry, B. A.; Gumbart, J. C. Redox-Driven Conformational Dynamics in a Photosystem-II-Inspired Beta-Hairpin Maquette Determined through Spectroscopy and Simulation. *J. Phys. Chem. B* **2017**, *121*, 3536−3545.
(27) Pagba, C. V.; Chi, S. H.; Perry, J.; Barry, B. A. Proton-Coupled Electron Transfer in Tyrosine and a Beta-Hairpin Maquette: Reaction Dynamics on the Picosecond Time Scale. *J. Phys. Chem. B* **2015**, *119*, 2726−2736.
(28) Pagba, C. V.; McCaslin, T. G.; Chi, S. H.; Perry, J. W.; Barry, B. A. Proton-Coupled Electron Transfer and a Tyrosine-Histidine Pair in a Photosystem II-Inspired Beta-Hairpin Maquette: Kinetics on the Picosecond Time Scale. *J. Phys. Chem. B* **2016**, *120*, 1259−1272.
(29) Martínez-Rivera, M. C.; Bruce, B. W.; Valentine, K. G.; Westerlund, K.; Hay, S.; Tommos, C. Electrochemical and Structural Properties of a Protein System Designed to Generate Tyrosine Pourbaix Diagrams. *J. Am. Chem. Soc.* **2011**, *133*, 17786−17795.
(30) Ravichandran, K. R.; Liang, L.; Stubbe, J.; Tommos, C. Formal Reduction Potential of 3,5-Difluorotyrosine in a Structured Protein: Insight into Multistep Radical Transfer. *Biochemistry* **2013**, *52*, 8907−8915.
(31) Glover, S. D.; Jorge, C.; Liang, L.; Valentine, K. G.; Hammarstrom, L.; Tommos, C. Photochemical Tyrosine Oxidation in the Structurally Well-Defined Alpha3Y Protein: Proton-Coupled Electron Transfer and a Long-Lived Tyrosine Radical. *J. Am. Chem. Soc.* **2014**, *136*, 14039−14051.
(32) Pagba, C. V.; McCaslin, T. G.; Veglia, G.; Porcelli, F.; Yohannan, J.; Guo, Z.; McDaniel, M.; Barry, B. A. A Tyrosine-Tryptophan Dyad and Radical-Based Charge Transfer in a Ribonucleotide Reductase-Inspired Maquette. *Nat. Commun.* **2015**, *6*, No. 10010.
(33) Barry, B. A.; Chen, J.; Keough, J.; Jenson, D. L.; Offenbacher, A. R.; Pagba, C. V. Proton Coupled Electron Transfer and Redox Active Tyrosines: Structure and Function of the Tyrosyl Radicals in Ribonucleotide Reductase and Photosystem II. *J. Phys. Chem. Lett.* **2012**, *3*, 543−554.
(34) Maupetit, J.; Derreumaux, P.; Tuffery, P. Pep-Fold: An Online Resource for *De Novo* Peptide Structure Prediction. *Nucleic Acids Res.* **2009**, *37*, W498−W503.
(35) Jo, S.; Jiang, W. A Generic Implementation of Replica Exchange with Solute Tempering (Rest2) Algorithm in NAMD for Complex Biophysical Simulations. *Comput. Phys. Commun.* **2015**, *197*, 304−311.
(36) Wang, L.; Friesner, R. A.; Berne, B. J. Replica Exchange with Solute Scaling: A More Efficient Version of Replica Exchange with Solute Tempering (Rest2). *J. Phys Chem. B* **2011**, *115*, 9431−9438.
(37) Devoe, H.; Tinoco, I., Jr. The Hypochromism of Helical Polynucleotides. *J. Mol. Biol.* **1962**, *4*, 518−527.
(38) Rhodes, D.; Burley, S. K. Protein-Nucleic Acid Interactions. *Curr. Opin. Struct. Biol.* **1997**, *7*, 73−75.
(39) Blanco-Rodriguez, A. M.; Towrie, M.; Sykora, J.; Zalis, S.; Vlcek, A., Jr. Photoinduced Intramolecular Tryptophan Oxidation and Excited-State Behavior of [Re(L-AA)$(Co)_3$(Alpha-Diimine)](+) (L = Pyridine or Imidazole, Aa = Tryptophan, Tyrosine, Phenylalanine). *Inorg. Chem.* **2011**, *50*, 6122−6134.
(40) Vivian, J. T.; Callis, P. R. Mechanisms of Tryptophan Fluorescence Shifts in Proteins. *Biophys. J.* **2001**, *80*, 2093−2109.
(41) Adams, P. D.; Chen, Y.; Ma, K.; Zagorski, M. G.; Sonnichsen, F. D.; McLaughlin, M. L.; Barkley, M. D. Intramolecular Quenching of Tryptophan Fluorescence by the Peptide Bond in Cyclic Hexapeptides. *J. Am. Chem. Soc.* **2002**, *124*, 9278−9286.
(42) Kandori, H.; Borkmann, R. F.; Yoshihara, K. Picosecond Transient Absorption of Aqueous Tryptophan. *J. Phys. Chem.* **1993**, *97*, 9664−9667.
(43) Sharma, B.; Asher, S. A. UV Resonance Raman Investigation of the Conformations and Lowest Energy Allowed Electronic Excited States of Tri- and Tetraalanine: Charge Transfer Transitions. *J. Phys. Chem. B* **2010**, *114*, 6661−6668.
(44) Gord, J. R.; Hewett, D. M.; Hernandez-Castillo, A. O.; Blodgett, K. N.; Rotondaro, M. C.; Varuolo, A.; Kubasik, M. A.; Zwier, T. S. Conformation-Specific Spectroscopy of Capped, Gas-Phase Aib Oligomers: Tests of the Aib Residue as a 3_{10}-Helix Former. *Phys. Chem. Chem. Phys.* **2016**, *18*, 25512−25527.
(45) Léonard, J.; Sharma, D.; Szafarowicz, B.; Torgasin, K.; Haacke, S. Formation Dynamics and Nature of Tryptophan's Primary Photoproduct in Aqueous Solution. *Phys. Chem. Chem. Phys.* **2010**, *12*, 15744−15750.
(46) Barry, B. A.; el-Deeb, M. K.; Sandusky, P. O.; Babcock, G. T. Tyrosine Radicals in Photosystem II and Related Model Compounds. *J. Biol. Chem.* **1990**, *265*, 20139−20143.
(47) Barry, B. A.; El-Deeb, M.; Sithole, I.; Debus, R.; McIntosh, L.; Babcock, G. T. Structural Studies of the Stable Tyrosine Radical, Y_D^+ in Photosystem II. In *Current Research in Photosynthesis*; Baltscheffsky, M., Ed.; Kluwer Academic Publishers: Dordrecht, 1990; Vol. *I*, pp 483−486.
(48) Reece, S. Y.; Stubbe, J.; Nocera, D. G. Ph Dependence of Charge Transfer between Tryptophan and Tyrosine in Dipeptides. *Biochim. Biophys. Acta, Bioenerg.* **2005**, *1706*, 232−238.
(49) Walden, S. E.; Wheeler, R. A. Distinguishing Features of Indolyl Radical and Radical Cation: Implications for Tryptophan Radical Studies. *J. Phys. Chem.* **1996**, *100*, 1530−1535.

DOI: 10.1021/acs.jpcb.8b12452
J. Phys. Chem. B 2019, 123, 2780−2791

(50) Shafaat, H. S.; Leigh, B. S.; Tauber, M. J.; Kim, J. E. Spectroscopic Comparison of Photogenerated Tryptophan Radicals in Azurin: Effects of Local Environment and Structure. *J. Am. Chem. Soc.* **2010**, *132*, 9030−9039.
(51) Stoll, S.; Shafaat, H. S.; Krzystek, J.; Ozarowski, A.; Tauber, M. J.; Kim, J. E.; Britt, R. D. Hydrogen Bonding of Tryptophan Radicals Revealed by EPR at 700 GHz. *J. Am. Chem. Soc.* **2011**, *133*, 18098−18101.
(52) Kim, S. T.; Sancar, A.; Essenmacher, C.; Babcock, G. T. Time-Resolved EPR Studies with DNA Photolyase: Excited-State FADH0 Abstracts an Electron from Trp-306 to Generate FADH-, the Catalytically Active Form of the Cofactor. *Proc. Natl. Acad. Sci. U.S.A.* **1993**, *90*, 8023−8027.
(53) Aubert, C.; Mathis, P.; Eker, A. P.; Brettel, K. Intraprotein Electron Transfer between Tyrosine and Tryptophan in DNA Photolyase from *Anacystis nidulans*. *Proc. Natl. Acad. Sci. U.S.A.* **1999**, *96*, 5423−5427.
(54) Waters, M. L. Aromatic Interactions in Model Systems. *Curr. Opin. Chem. Biol.* **2002**, *6*, 736−741.
(55) Mahalakshmi, R.; Raghothama, S.; Balaram, P. NMR Analysis of Aromatic Interactions in Designed Peptide Beta-Hairpins. *J. Am. Chem. Soc.* **2006**, *128*, 1125−1138.
(56) Tatko, C.; Waters, M. L. Comparison of C-H Pi and Hydrophobic Interactions in a Beta Hairpin Peptide: Impact on Stability and Specificity. *J. Am. Chem. Soc.* **2004**, *126*, 2028−2034.
(57) Popp, A.; Wu, L.; Keiderling, T. A.; Hauser, K. Effect of Hydrophobic Interactions on the Folding Mechanism of Beta-Hairpins. *J. Phys. Chem. B* **2014**, *118*, 14234−14242.
(58) Burley, S. K.; Petsko, G. A. Aromatic-Aromatic Interaction: A Mechanism of Protein Structure Stabilization. *Science* **1985**, *229*, 23−28.
(59) Minnihan, E. C.; Nocera, D. G.; Stubbe, J. Reversible, Long-Range Radical Transfer in *E. coli* Class Ia Ribonucleotide Reductase. *Acc. Chem. Res.* **2013**, *46*, 2524−2535.
(60) Krebs, C.; Chen, S.; Baldwin, J.; Ley, B. A.; Patel, U.; Edmondson, D. E.; Huynh, B. H.; Bollinger, J. M. Mechanism of Rapid Electron Transfer During Oxygen Activation in the R2 Subunit of *Escherichia coli* Ribonucleotide Reductase. 2. Evidence for and Consequences of Blocked Electron Transfer in the W48F Variant. *J. Am. Chem. Soc.* **2000**, *122*, 12207−12219.
(61) Barry, B. A.; Babcock, G. T. Tyrosine Radicals Are Involved in the Photosynthetic Oxygen-Evolving System. *Proc. Natl. Acad. Sci. U.S.A.* **1987**, *84*, 7099−7103.
(62) Dekker, J. P.; Gorkom, H. J. V.; Brok, M.; Ouwehand, L. Optical Characterization of Photosystem II Electron Donors. *Biochim. Biophys. Acta, Bioenerg.* **1984**, *764*, 301−309.
(63) Gerken, S.; Brettel, K.; Schlodder, E.; Witt, H. T. Optical Characterization of the Immediate Donor to Chlorophyll A_{ii}^{+} in O_2-Evolving Photosystem II Complexes. *FEBS Lett.* **1988**, *237*, 69−75.
(64) Sweeney, J. A.; Asher, S. A. Tryptophan UV Resonance Raman Excitation Profiles. *J. Phys. Chem.* **1990**, *94*, 4784−4791.
(65) Woody, R. W. Contributions of Tryptophan Side Chains to the Far-Ultraviolet Circular Dichroism of Proteins. *Eur. Biophys. J.* **1994**, *23*, 253−262.
(66) Callis, P. R. ^1L_a and ^1L_b Transitions of Tryptophan: Applications of Theory and Experimental Observations to Fluorescence of Proteins. *Methods Enzymol.* **1997**, *278*, 113−150.
(67) Kosinski-Collins, M. S.; Flaugh, S. L.; King, J. Probing Folding and Fluorescence Quenching in Human GammaD Crystallin Greek Key Domains Using Triple Tryptophan Mutant Proteins. *Protein Sci.* **2004**, *13*, 2223−2235.
(68) Sharma, D.; Leonard, J.; Haacke, S. Ultrafast Excited-State Dynamics of Tryptophan in Water Observed by Transient Absorption Spectroscopy. *Chem. Phys. Lett.* **2010**, *489*, 99−102.
(69) Ovejas, V.; Fernandez-Fernandez, M.; Montero, R.; Castano, F.; Longarte, A. Ultrafast Nonradiative Relaxation Channels of Tryptophan. *J. Phys. Chem. Lett.* **2013**, *4*, 1928−1932.
(70) Müller, P.; Ignatz, E.; Kiontke, S.; Brettel, K.; Essen, L. O. Sub-Nanosecond Tryptophan Radical Deprotonation Mediated by a Protein-Bound Water Cluster in Class II DNA Photolyases. *Chem. Sci.* **2018**, *9*, 1200−1212.
(71) Reece, S. Y.; Nocera, D. G. Proton-Coupled Electron Transfer in Biology: Results from Synergistic Studies in Natural and Model Systems. *Annu. Rev. Biochem.* **2009**, *78*, 673−699.

DOI: 10.1021/acs.jpcb.8b12452
J. Phys. Chem. B 2019, 123, 2780−2791